UNIVERSITY OF TWENTE.

micronit

University of Twente and Micronit

Thesis report

Biomedical Engineering

15-08-2023

Hot embossing microstructures onto thermoplastic elastomer membranes using micromilled and glass etched moulds for the use in downscaling upscalable microfluidic elements.

Author:
T.J. de Jager s1990977

Under supervision of:
prof.dr.ir. L.I. Segerink
senior RD scientist S. Meucci
Researcher J.T. Loessberg-Zahl

1 Abbreviations and acronyms

TPE (Thermoplastic elastomer)
PS (Polystyrene)
PC (Polycarbonate)
IPA (Isopropyl alcohol)
HF (hydrofluoric acid)
SiO2 (silicone dioxide)
Tg (glass transition temperature)

2 Abstract

Hot embossing is a manufacturing method which has potential for large scale industrial production for microfluidic devices. The goal of this research was to hot emboss microstructures onto thermoplastic elastomer membranes using different kinds of mould. These microstructures include Quake valves and check valves in arrays, and a fluidic rectifier and dampeners as additional features. This research succeeded in replicating microstructures on thermoplastic elastomer membranes, with open discussions over some differences observed between the replica and the design. Channel width and height characterisation has been performed on the Hot embossed membranes and the moulds. The moulds were manufactured by casting PDMS on a glass etched negative of the mould, and by micromilling. A single complete stack was manufactured and fluidic priming was tested. The defects in fluidic and pneumatic functionalities were documented and discussed. This research shows the compatibility of industrializable materials and processes used with the fabrication of active pneumatic elements, and sheds light on the first line of issues that need to be addressed to progress this further.

2.1 Nederlandse samenvatting

Warmte embossen is een productie methode welke potentie heeft voor industriële applicatie, op een grote schaal, voor microfluïdische hulpmiddelen. Het doel van dit onderzoek was om thermoplastische elastomeer membranen te embossen met gebruik van verschillende soorten mallen. De microstructuren bevat Quake valves en check valves in rijen, en een fluïdische gelijkrichter en dempers als overige structuren. Dit onderzoek is geslaagd in het repliceren van microstructuren op thermoplastische membranen, met een open discussie over verschillen tussen de replica en het ontwerp. The kanaal breedte en hoogte karakterisatie is volbracht op de warm embossed membranen en de mallen. De mallen waren geproduceerd door PDMS of een glas geëtste negatief te gieten, en met behulp van micromilling. Een enkele complete stack was geproduceerd en fluïdische actuatie samen met microscopisch onderzoek liet zien dat de twee kanten van het membraan met elkaar verbonden waren wat impliceerde dat er problemen waren met het binden van de lagen. Dit onderzoek laat de compatibiliteit van industrieel op te schalen materialen en processen zien met het fabriceren van actieve pneumatische elementen, en geeft inzicht op de eerste lijn van problemen welke moeten worden geadresseerd voordat progressie mogelijk is.

Contents

3 Introduction

A cutting edge field of medicine is personalised medicine. Creating personalised treatments requires high volume production and reliability. Crucial for personalised medicine are methods of testing which are reproducible and can be manufactured in high quantities. One of the field with most potential to solve this matter is the field of microfluidics. Microfluidics is used in the field of bioengineering focused on the control of fluid flow in structures which are micron sized like channels, chambers, valves and more. The goal is to produce reproducible chips with a wide variety of functions. In microfluidics, a common method of controlling the fluid's flow is using pressure pumps and regulators. This is often applied in combination with valves. A valve is a fluidic construct enabling control over the flow of fluids by varying the resistance of a channel, opening or closing it. A valve is constructed into microfluidic devices to enable more fine tuned control. Microfluidic valves and other fluid control elements can also be used, often together in networks, to automate workflows. A study has shown the capability of microfluidic elements in creating chips which have pumps and mixers [1].

3.1 Quake valves

One of the most common valve in microfluidics is called a Quake valve[2]. A Quake valve is a combination of two channels with a membrane in between. The membrane displaces into one of the channels when pressure is applied to the other. The membrane displaces into the channel below and closes it.
There is a way to classify different kinds of microfluidic valves. They can be divided into normally open or closed valves. As the name might suggest the difference is if the valve allows flow through since the fluidic channel is open in absence of pneumatic over pressure. When pressure is applied to the pneumatic channel, a deformable membrane is pushed into a channel below. Quake valves are for example normally open valves as shown below1.

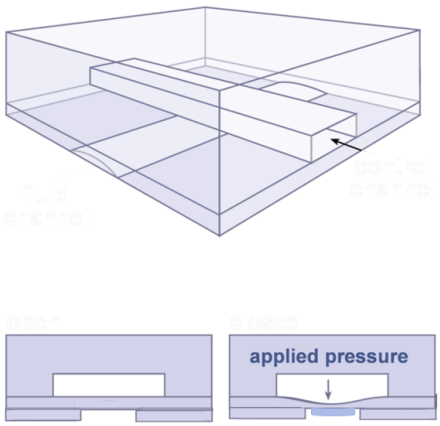

Figure 1: This figure shows a side view and a cross section of a Quake valve with the arrow pointing at the membrane displacement into the channel below.[3]

A normally closed valve does not allow flow through the valve unless the pneumatic channel is actuated. A moving part of the valve needs to be pulled or pushed away for the valve to open.

This can for example be done by using pressure regulators to apply negative pressure in the pneumatic channel pulling a deformable structure into it. An example of this is shown below in figure 2.

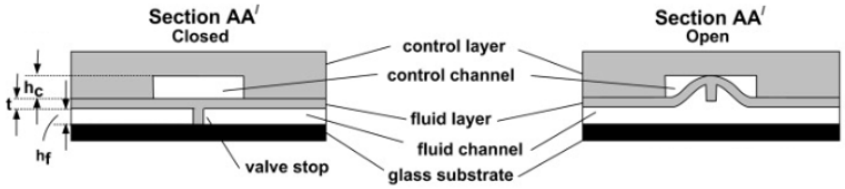

Figure 2: This figure shows a cross section of a normally closed valve[4].

Multiple Quake valves can also be combined into simple structures on their own. A simple peristaltic pump uses three valves in tandem to produce flow for example. This is shown below in figure 3.

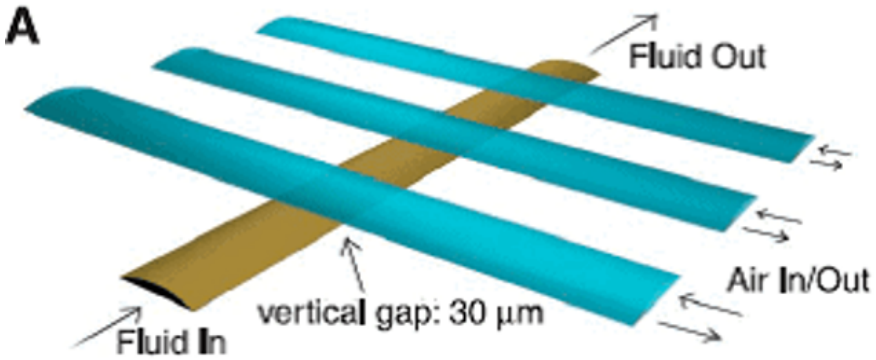

Figure 3: This figure shows a peristaltic pump which is made out of three Quake valves. [2].

A peristaltic pump can be made from different types of valves. An example is shown in figure 4 with circular vertical valves[5].pla

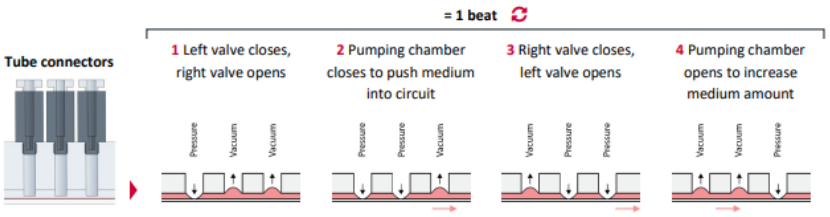

Figure 4: This figure shows a peristaltic pump which is made out of three circular valves. [5].

3.2 Manufacturing methods

Normally open valves can be made in a multitude of ways. Some common methods include photolitohography, micromilling, PDMS casting and hot embossing.

3.2.1 Photolithography

Photolithography is a general term for the use of light to produce accurately patterned thin films of resist material over a substrate, like for example a silicon wafer or SU-8. Patterned thin films are used to protect selected areas of it during subsequent processing, like etching or deposition. This will then create microstructures which can result in valves such as Quake valves. The pattern on the thin film can be a negative or a positive of the desired structures according to the subsequent processing step which is used. A positive means that the mask only does not cover the intended structures. An example of this is UV-photolithography, which uses a mask to block UV light from the intended structures, cross linking a prepolymer where UV light passes the mask.
A negative implies that the pattern covers the intended structures. Subsequent manufacturing steps like PDMS casting can then take the negative and use it as a mould to arrive at the intended structure.

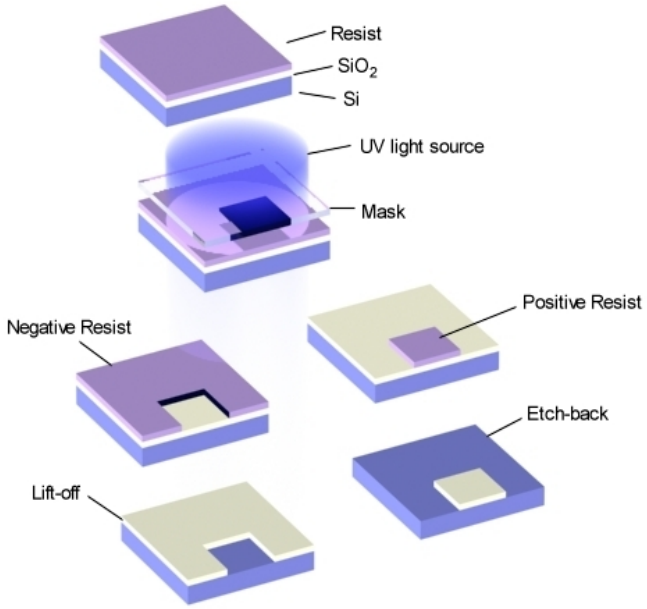

Figure 5: This diagram shows a simple step by step for UV photolithography using both a negative resistant and a positive resist.[6].

Photolithography is a manufacturing method which has high precision and can produce microfluidic structures only limited to the details of the mask and the wavelength of the UV light (in the range of 254-365 nm). The process does have difficulties when trying to produce microfluidic structures with multiple layers, as stacking of multiple layers seems to be one of the only few options with its own limitations.

3.2.2 PDMS casting

PDMS casting uses a negative mould which has the wanted structures on its topography. The PDMS prepolymer is mixed with its cross-linker, after which the mixture is added on top of the negative mould in a surrounding frame. This frame allows the PDMS mixture to fill the created cavity. The PDMS are the structures now transferred from the negative mould onto the PDMS after baking and hardening. This process is shown below using a 3D printed mould, but the mould can be manufactured in many ways including glass etching, 3D printing, micromilling or lithography.

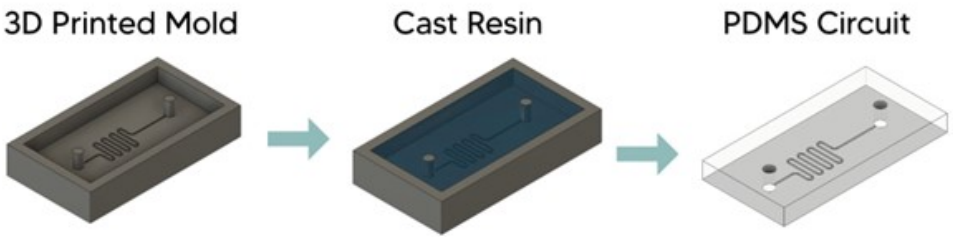

Figure 6: This diagram shows the process of PDMS casting creating a PDMS circuit chip. [7].

PDMS casting as a manufacturing method is reliable and easy to handle. Limitations for PDMS casting are the need for a mould for structuring and that removing the mould and frame from the PDMS, if not coated properly, can prove to be difficult.

3.2.3 Micromilling

Micromilling is another manufacturing methods as mentioned before. Micromilling uses a precision drill to carve out structures from a stock material. The precision drill can use a variety of shaped drills to carve out channels, chambers and inlets using programmed instructions in a repeatable manner.

3.3 Hot embossing

Quake valves are widely accepted, but have their limitations. It has been shown that Quake valves can be made with a density of up to 1.000.000 valves/cm^2 [8][9], which means that high volume integration of these valves has been shown to be possible. However the researches which include that level of high volume integration just includes high density woven Quake valves and little to no higher microfluidic tech integration.

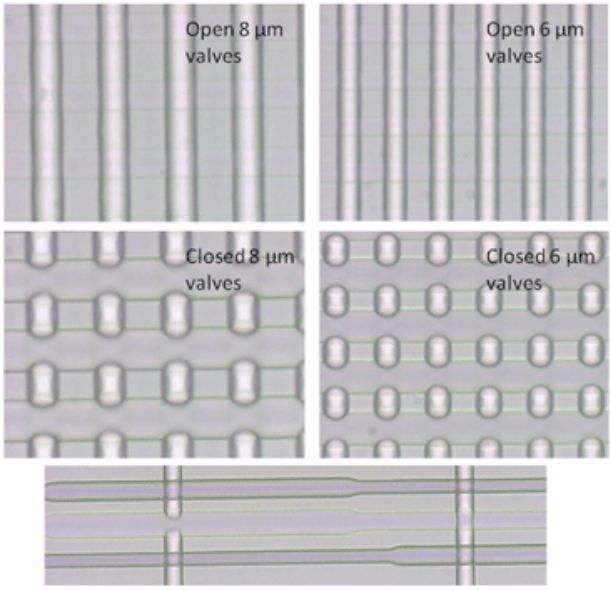

Figure 7: This image shows Quake valves opening and closing at a density nearing 1.000.000 valves/cm^2[8].

From literature it becomes apparent that this high density integration of the Quake valves have been published since 2012, and this has not been shown to be applied to products for the market. More intricate designs including Quake valves have been shown to work, like for example the Wyss Institute's Octobot, an entirely soft autonomous microfluidic robot [10][11]. This research shows great use of intricate microfluidic circuits, but has no high density integration of valves. Past researches have shown industry that the concept and use of these types of valves is possible, but large scale integration into industry is yet to be seen. The methods with which the high density Quake valves[8] or the Octobot [10][11] manufacture their designs are PDMS casting and 3D printing, both methods which are hard to translate high scale production for industry. Research has shown that there are methods which use soft materials and membranes with milled channels that are able to be upscaled into industry[12][13], but they do not allow for the miniaturized valves this research is aiming for.

A method with potential for industry is hot embossing. Hot embossing uses thermoplastics on a mould and such a method can easily be repeated and applied to large volume production. One of the goals of this research is to create down scaled microfluidic structures with a method capable of being upscaled into industry. The method chosen is a combination of micromilling and structures which are hot embossed into a TPE (Thermoplastic Elastomer) membrane.

Hot embossing is a micro-fabrication technique in which micron-scale structures on a mould are replicated on to a polymer substrate by the application of pressure and heat[14]. This is commonly done by using a hot press [15] to both heat up and press down onto a mould, which can be manufactured in different methods but needs to be heat resistant.

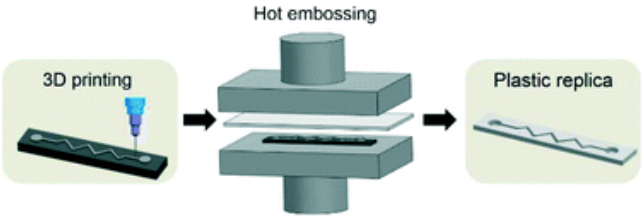

Figure 8: This figure shows the simplified steps of Hot embossing microfluidic chips with a 3D printed mould [16].

Fig 8 shows a parallel plate architecture, but there are also more intricate ways to perform the embossing such as using hot roller embossing[17]. There are also different variations of hot embossing to increase the cycle time or to apply non-uniform pressure distribution like gas-pressurized embossing, ultrasonic hot embossing, inductive hot embossing, laser assisted hot embossing[17], etc.
There is another practical issue why hot embossing the structures into the membrane of the Quake valve is a good idea. As the depth of the channel, which is able to close, becomes relatively smaller than the membrane's thickness, it becomes increasingly more difficult to displace the membrane into a channel enough to close it off. If lets say a membrane of 100μm tries to displace into a 50μm channel, the flexibility of the TPE (thermoplastic elastomer) might not be enough to completely close the channel. This research aims to use Hot embossing to manufacture microfluidic channels and valves which structures are partially embedded as indentations in a 100 μm TPE membrane. The channel which is to be able to close in a Quake valve is now an indentation in the TPE. The TPE will displace and the embedded channel will collapse into itself closing the flow through the channel completely when pressure is applied in the pneumatic channel will . Which bring us to the goal of this research: to hot emboss microstructures onto TPE membranes using different kinds of moulds applied on down scaling upscalable microfluidic elements.

Quake valves are common in microfluidics but of course there are many other types of flow control elements. This research aims to apply the same methods of hot embossing microstructures on a TPE to create Quake and check valves and describe other elements like dampeners or a fluidic rectifier[18].

4 System design

4.1 Concept

The goal of this research as mentioned in section 3, is to create microstructures in a deformable membrane to make small valves that can be made by the industrially usable process of embossing. In this case industrially usable implies a process which can be upscaled and mass produced using the repeatable method of hot embossing.

When trying to create small Quake valves in thermoplastics an issue arises as the ratio between the thickness of the membrane and the depth of the channel becomes too deep. The thicker the membrane is opposite to the depth of the channel, the more difficult it is to have the membrane push into the channel. This is shown in figure 9 [a] below.

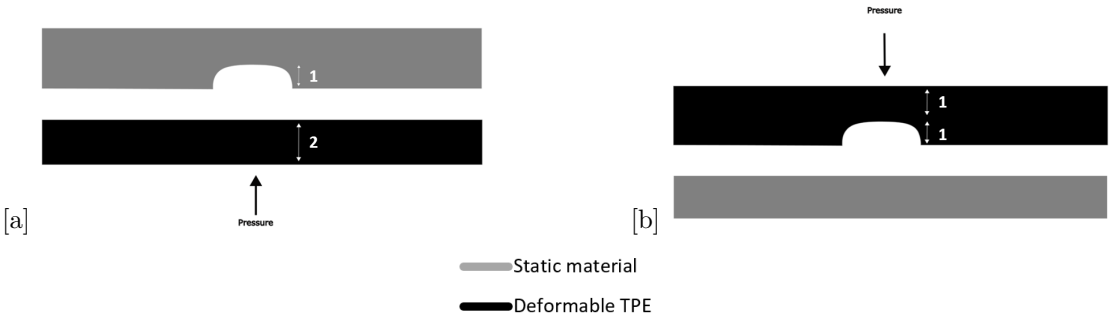

Figure 9: Two diagrams with [a] exhibiting the size difference between a channel and a membrane causing difficulties displacing the membrane into the channel, and [b] a diagram exhibiting the method of closing the embossed channel using pressure.

The size difference causes the membrane to not be fully able to be pushed into the channel. To counter this issue, channel structures will be embedded into a TPE which allows the membrane to close onto itself instead of needing to be pushed into a channel below. This will allow the channel to be downscaled and this concept is shown above in figure 9 [b]. This in combination with hot embossing being a very upscalable method for production brings the system concept to an upscalable manufacturing method for Quake valves in thermoplastics.

Current researches uses a variety of manufacturing methods for their microfluidic valves. A simple overview of these different manufacturing methods and their features is shown below.

fabrication method	minimum feature size	average area used	usability for this research
UV Lithography [19]	365 nm or more	2000 cm^2	high precision, not upscalable
Micromilling [20]	10 μm	2000 cm^2 (machine dependent)	precise, flexible, use in mould and plates
3D printing [21]	7.5 μm	Table and setup dependent	flexible, not precise enough

Next to manufacturing methods there are also methods to transfer microfluidic features between processing steps. Examples are masks for lithography or etching and moulds for .

Transfer method	minimum feature size	average area	usability
Hot embossing [14]	10 μm	machine specific	precise, reproducible, use in membrane features
Glass etching [22]	5 μm	2000 cm^2	precision, smooth curves, use for negative mould
PDMS casting [23]	5 μm	mould specific	easy precise method, use for transferring from glass mould

Micromilling and glass etching were chosen as the methods for creating the moulds used in this research. The other manufacturing or transfer methods were not used due to the mentioned limitations. The glass etching was not the process with which the mould was manufactured, but rather transferred from the mask unto the glass. This mask was ordered at an external company from the Solidworks design.

The embossed features will come from the use of moulds which have been manufactured by glass etching and micromilling. The structures were transferred after embossing a 100 μm membrane onto these mould with 50 μm features.
A bottom PS plate was used to close off the embossed channels. This plate does not need any fluidic features but included alignment features for visual alignment and pinholes for physical alignment. On the other side of the membrane there needs to be another chamber or channel to apply the pneumatic pressure to close the Quake valves. This research used micromilled PS channels. Both sides of the valve could be theoretically embossed, but this research will first aim at one side of the valve being embossed. This concludes the concept in a three layer stack of a top PS plate with fluidic inlets on one side and pneumatic channels on the other, an embossed TPE with features on one side and a bottom PS plate without any valve features.

4.2 SolidWorks design

After the concept, the first step is creating a SolidWorks design for fabrication of the mould used for embossing the TPE. A replica of the combined layers and of the mould was designed. Central in the 6inch wafer are three microscope slide sized arrays. This size was chosen for the ease of using the chips as its the same size as a standard glass slide.

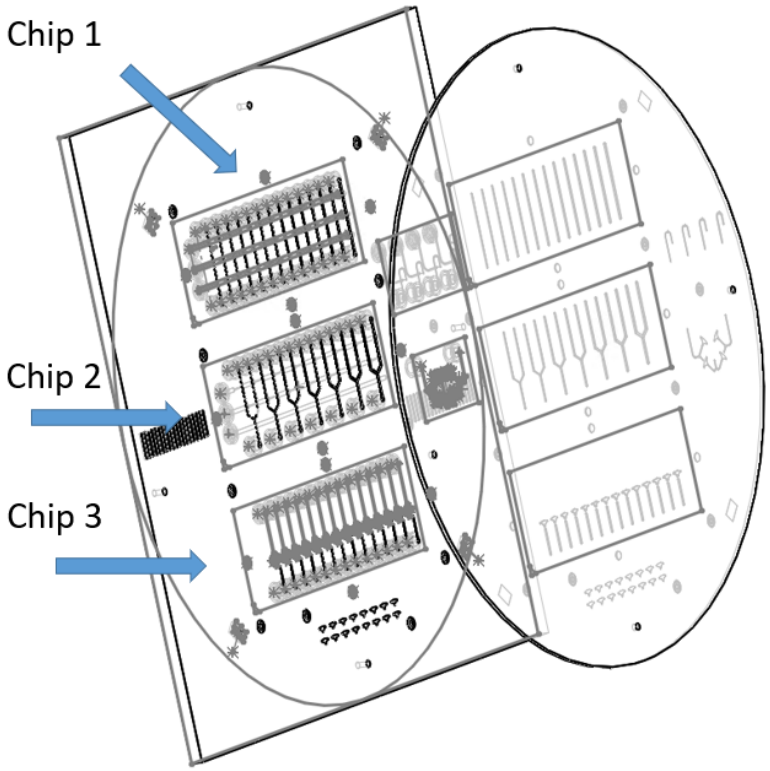

Figure 10: An image portraying a tilted view of the replica (left) and the mould (right) in SolidWorks.

4.2.1 Three array chips

The first and second chip have 3 horizontal pneumatic lines in the PS layer and 14 vertical embossed channels within the TPE membrane. The vertical and horizontal channels are connected with tubing to a pressure controller. The variable in the array of the first chip is the width of the vertical fluidic channels. The aim of this chip is to characterise the closing and opening of Quake valves with different sized overlap between the pneumatic and the fluidic channels. The wider the fluidic channel, the more surface area there will be and the more the actuation of the pneumatic channel will cause the membrane to displace. The widths of the embossed channel range between 110 and 550 μm in width increasing in equal increments of 31.4 μm. These sizes were chosen by the limitations of the glass etched mould. The glass etched channel was at least twice the depth of the channel, which was 50 μm, as it is an isotropic process. Leaving enough material for the mask causes the smallest fluidic channel to have a chosen width of 110 μm. To enable the use of the Quake valves and channels as a peristaltic pump 3 pneumatic lines are used.

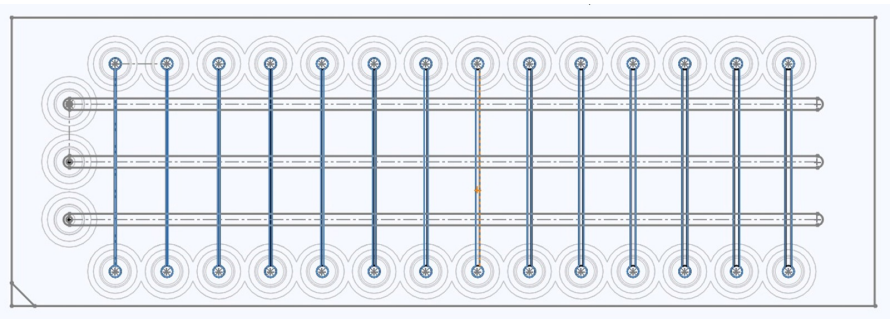

Figure 11: This figure shows the first chip with an array of channels with a width between 110 and 550 micron width.

On the second chip it was decided that the embossed channels would form a Y-shape with the variable being the width of the embossed channels ranging between 110 and 550 micron in width increasing in equal increments of 31.4 μm. The Y-shape for this array was chosen to be able to make a selection between two converging channels, either choosing which of two substances gets to the outlet or choosing if one substance goes to one outlet, to the other or splits between the two. The Y-shape channels can also be tested with colorant for visualisation purposes, as using colorant and switching the pneumatic actuation could lead to selective mixing of colours.
The first 2 pneumatic channels are shaped differently with the goal to multiplex control over the channels without using difficult routing of pneumatic channels to not cross the fluidic channels. The first 2 pneumatic channels are thinned around one of the fluidic channels of the Y-shapes. Theoretically, the smaller the pneumatic channel with respect to the fluidic channel, the less it will close[1] as the surface area between the two channels becomes less. This should prevent the TPE to displace completely into the fluidic channel, allowing flow through and in such selectively keeping that fluidic channel open.

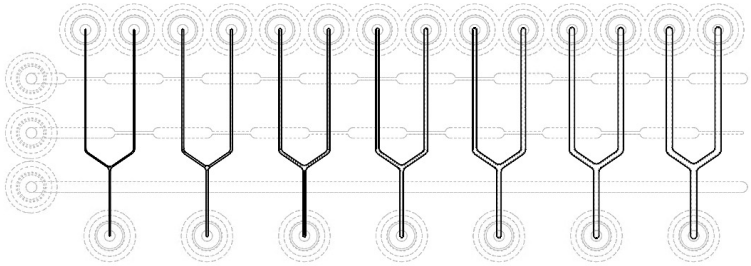

Figure 12: This figure shows the second chip with an Y-array of channels with a width between 110 and 550 μm width.

The third chip holds an array with check valves. Check valves are valves which allow flow through one way but not the other way often with the use of a moving membrane[24][25]. This is referred to as forward and backward flow. The designed check valves are moon-like shaped and shown in more detail below. The 14 check valves are divided up into experimenting with different features of the moon shape, which division is listed below.

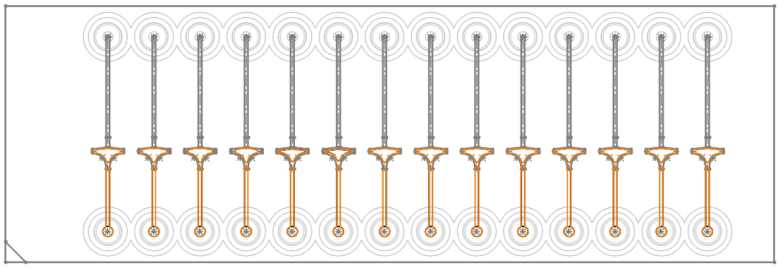

Figure 13: This figure shows the third chip with a multitude of check valves.

1. 4 moon shape widths
2. 2 moon shape heights
3. 5 different length of the skip
4. 3 extra standard sized for use in different sized slits

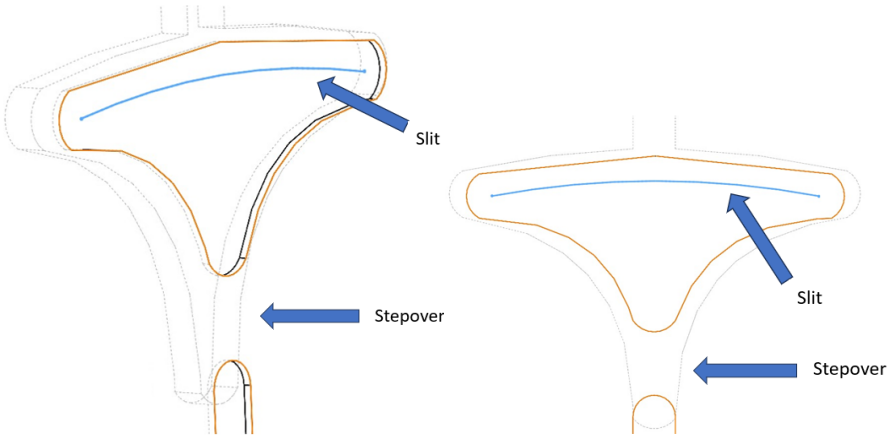

Figure 14: This figure shows an angled view (a) and a top view (b) of the check valve.

Shown in figure 14 (a) is an angled view of the sketch defining the edges of the embossed chamber. The moonshape in orange is the embossed side, and what can be seen is that between the moon shape and the channel there is a "stepover" where there is no channel. What can be seen in figure 14 is that the milled chamber below does cover the area where the stepover is. This stepover is used to enable better closing of the check valve. The fluid will pass through the membrane in a curved cut shown in figure 14 as a blue line. This will be cut using a drag knife on the NEO milling machine. A drag knife is a knife which is able to turn towards the direction the knife is pulled, allowing for clean cuts following a pattern programmed for the micromilling machine.

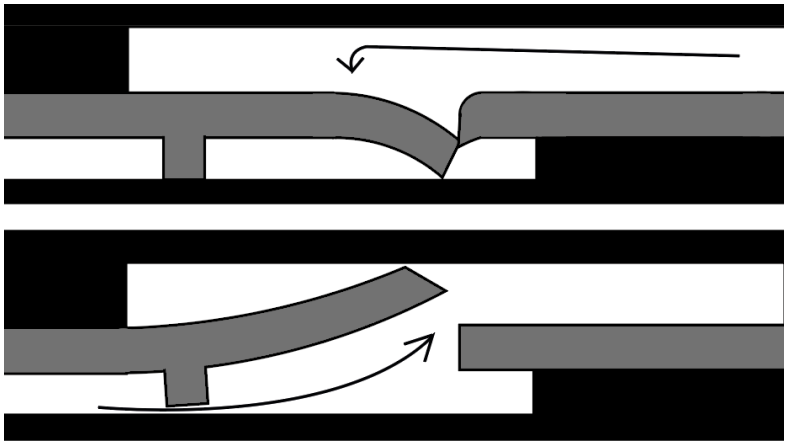

Figure 15: This diagram shows the cross section of the check valve design when pressure is applied closing it above or opening it below.

Figure 15 above shows how the check valve closes with the aid of the stepover. When pressure is applied forward through the check valve will the stepover and the TPE open up into the chamber below allowing flow through. The pressure will push down the TPE when the flow is backwards over the check valve. The stepover then, as the protruding feature, functions as a barrier.

4.2.2 Additional structures

Next to the central three arrays there are additional structures on the sides of the wafer.

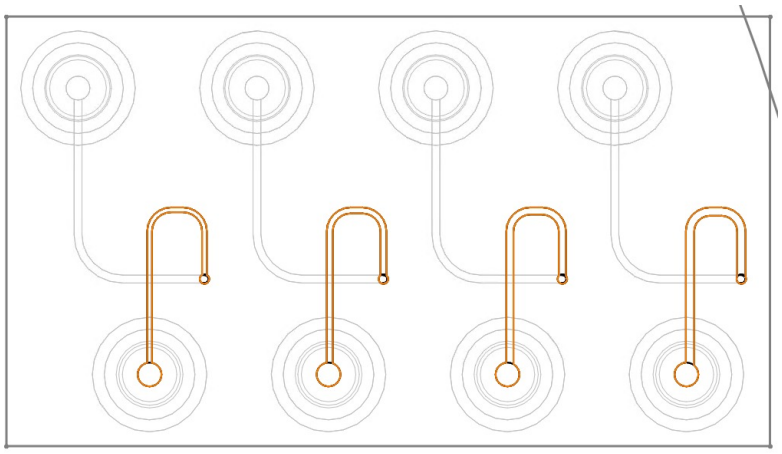

Figure 16: This figure shows an array of dampeners with widths ranging between 110 and 550 in width increasing in equal increments of 146 μm.

The additional structure shown above in figure 16 is a small array of dampeners with the widths of the channels ranging between 110 and 550 micron. As the embossed channel crosses the connected micromilled channel, when non-constant flow is applied to the dampener the pressure will partly close the channel below dampening the pressure peaks. This will increase the impedance. There

was no modelling or calculations done for the impedance, so till testing it will remain unclear if the impedance increase is big enough to cause dampening.

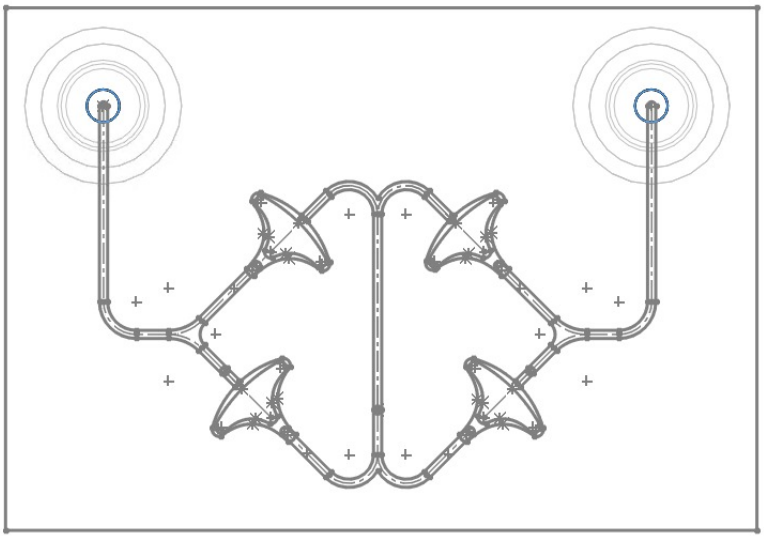

Figure 17: This figure shows a fluidic rectifier made from the same moonshaped check valves.

A famous circuit in electrical engineering is called a Wheatstone bridge and is commonly used to accurately measure unknown resistance forces or calibrating equipment[18]. In microfluidics a similar concept can be applied using check valves as diodes instead of impedance, called a fluidic rectifier. The basic principle is that no matter which the direction the flow is between the two inputs, due to the nature of the check valves, flow passes the middle vertical channel always in the same direction. This concept is called a fluidic rectifier[26]. This is an useful application of a check valve used commonly in recreating unidirectional flow through cell chambers for for example emulating blood flow.

4.2.3 alignment features

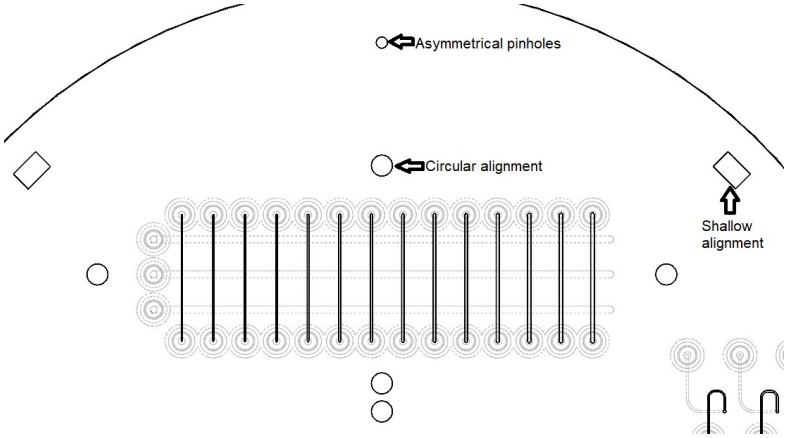

Figure 18: This figure shows a part of the replica with all 3 different alignment features.

Figure 18 above shows a part of the replica which includes the 3 different alignment features. Firstly there are small asymmetrical pinholes used for assembly. This is shown in figure 18 at the very top. Then at the edges of chip one there are circular alignment features. These circular alignment features are designed in both the top and bottom PS plate and the TPE with slightly different diameters. These alignment features allow more control and vision on the alignment of each individual structure. Lastly there are 4 square pockets in the diagonal corners of the design. These pockets are of a specific size which allows the use of a "shallow alignment" program designed by Micronit. This allows the micromilling machine to allign on these shallow pockets pockets in the diagonal corners of the design. These are used for the alignment of the TPE for cutting with the drag knife.

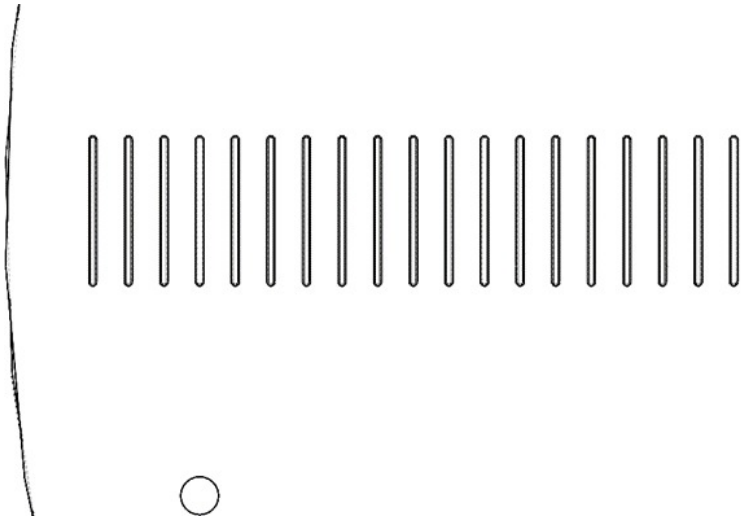

Figure 19: This figure shows a small array of lines as a ruler.

As the method of Hot embossing the TPE has been known to cause the materials to expand and contract due to the temperature changes, a "ruler" was added. This ruler is an array of straight lines near the edge. This is to check how homogeneous the division of the structures are due to the shrinking/expanding during the hot embossing process.

5 Materials and methods

5.1 Micromilling

For the top and bottom PS plates and one of the moulds, micromilling was used to mill the microstructures. This was done using the SolidCam software extension to generate the code needed for milling. Milling was done using a high speed CNC machine (Datron Neo [20]) on PS 6-inch-wide plates. The Datron Neo machine uses a toolbox which allows to load up to 24 tools, and can automatically switch them during milling procedure. Different tools can be added to the drill head by hand, like a drag knife or elongated tools.

The mould was first produced in PS and then in PC (polycarbonate). PS is easier to micromill leaving less burring while PC has the necessary heat resistance, denoted as Tg (glass transition temperature), for the hot embossing process. Tg defines at what temperature the base material changes from a hard/glassy state to a soft state[27]. The Tg of PC is around 147 degrees Celsius[28] and the Tg of PS is around 100 degrees Celsius[29]. PC is a viable option as the TPE used in this research is embossable above 100 degrees Celcius, but the PS will reach its Tg and become mechanically unstable.
The PS/PC plates were first cleaned with IPA (isopropyl alcohol) and lined with a protective layer of plastic. The plates are then suction stuck to the milling table. The exact coordinates of the plate were defined using an embedded probe system and subsequently the milling was performed. This research used micromilling not only for the mould but also as for micromilled plates above and below the TPE in PS. For the moulds and the bottom PS plate only one side was milled but for the top PS plate both sides were milled in separate instances. The TPE was cut with the same machine using a drag knife. To define the coordinated of the TPE for the milling machine a "shallow alignment" program was used. This is a program used by Micronit which uses the built in probe system of the milling machine to align on very shallow features.

5.2 Glass etching and PDMS casting

For the second mould it was decided to use the glass etching production Micronit had in place. The design was converted into a Clewin file [30] after which a photolithographic mask needed for glass etching in HF (hydrofluoric acid) was ordered from an external manufacturer. The production of the etched glass was performed by the production team of Micronit in their cleanroom in the High-Tech-Factory. The glass etching results into a negative of the mould.
The etched negative was then coated using a standard protocol from Micronit to avoid the PDMS sticking to the glass. PDMS was then casted onto the negative using a casting frame to create the same 6inch size around the glass negative after the glass etched negative was coated to prevent adhesion to the PDMS. The PDMS cure and prepolymer are mixed in a ratio of 1:10 respectively and soft baked at 65 degrees for 4 hours and hard baked at 200 degrees for 1 hour.

5.3 Characterisation of intermediary parts

In between the production steps of the different PS plates, PC plates, TPE membranes and etched glass characterisation was done to check the width and depth of the channels. The width of the channels was characterised using a Research Stereo-microscope System SZX16[31] with Olympus stream image and video analysis software[32]. The depth of the channels was characterised using a Quickvision Profilometer [33]. This profilometer works by using the focussing of a scope on different planes. The height the microscope in the profilometer moves to focus between

two planes is the same depth difference the planes have. The machine applies this principe and can be used either by hand or by creating a simple instruction program to focus on the different planes and display the height difference. The QV profilometer was in some cases not producing consistent results. When repeated qualatitive reapeted measurements were taken on the same features it produced very different results. A hand profilometer was used in those cases. This was a small electrical device which has a stick which can be pushed in. The electrical device accurately measures how far the stick is pushed in. This device is then mounted just above a microscope's table. When the microscope is then focussed on the two different planes of interest can the distance between the two planes be calculated by subtracting the two measurements of the device.

Both the width and the depth measurements were done on different parts of the channels on each chips. In chip 1 and 2 one measurement near the top and one near the lowest part of the channels was taken. For the Y shape channels in chip 2 four measurement were taken at each branch and the middle of the Y shape. This concludes in 56 measurement points.

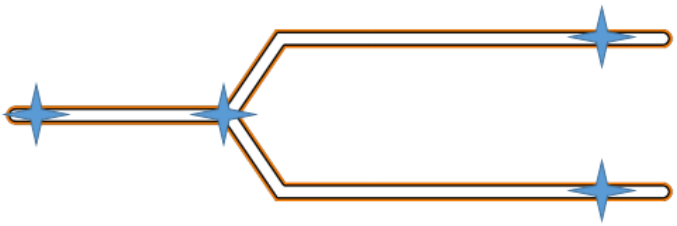

Figure 20: This figure shows the chosen locations for width and depth measurements for the Y-shaped channels.

5.4 Hot embossing

The hot embossing was performed using a hot press. The hot press transfers heat and pressure between two metal plates. As protection slates of rubber and white heat resistant cloth is used above and below the mould and the TPE. This was done in a 5 step process.

1. T0 ($\approx$ RT) and no pressure
2. T1 (>Tg) and no pressure for X1 seconds
3. T1 and P1 pressure for X2 seconds
4. T2 (<Tg) and P1 pressure for X3 seconds
5. T0 and P1 pressure for X4 seconds

The TPE was then carefully removed from the mould.

5.5 Shallow alignment and drag knife.

The embossed TPE now has the features of the channels and chambers, but it still needs to allow fluid to pass the membrane at the inlets and check valves. For this a drag knife was used attached to the drill of the NEO micromilling machine. The drag knife is able to rotate around its vertical axis allowing the knife to rotate and follow the milling machines movements. The micromilling machine needs to define the coördinate system of whatever stock it is working on. For the micromilling machine to be able to cut the circular holes it needed to be able to do this on the features on the embossed TPE. For this a tool was used which was developed at Micronit to align on shallow embossed features using the touch probe of the Neo. It uses a set program with the 1mm touch probe which the machine is equipped with to align on square pockets in 4 corners of the sample.

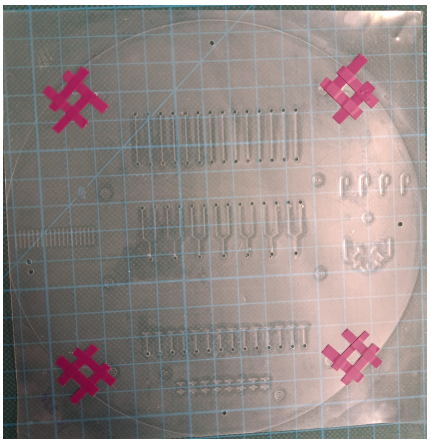

Figure 21: This image shows the taping of the corner pockets to increase the height of the pocket edges to ease the use of the shallow alignment tool.

The drag knife tool was then added to the milling machine and the turning of the drill head piece was turned off in the code for the milling. The machine is then given instructions to follow the generated instructions and drag the knife.

5.6 Stack assembly

The two PS plated and the TPE were aligned using the pinholes and circular alignment features. Both the PS plates are first coated using gas deposition using a standard program from Micronit. The assembly starts with the top PS plate on which first the TPE and then the bottom PS plate are places. The TPE is applied to an expansion ring with a plastic film which has a 6 inch circle cut out. Only the corners of the square TPE are attached to the plastic film in the expansion ring.

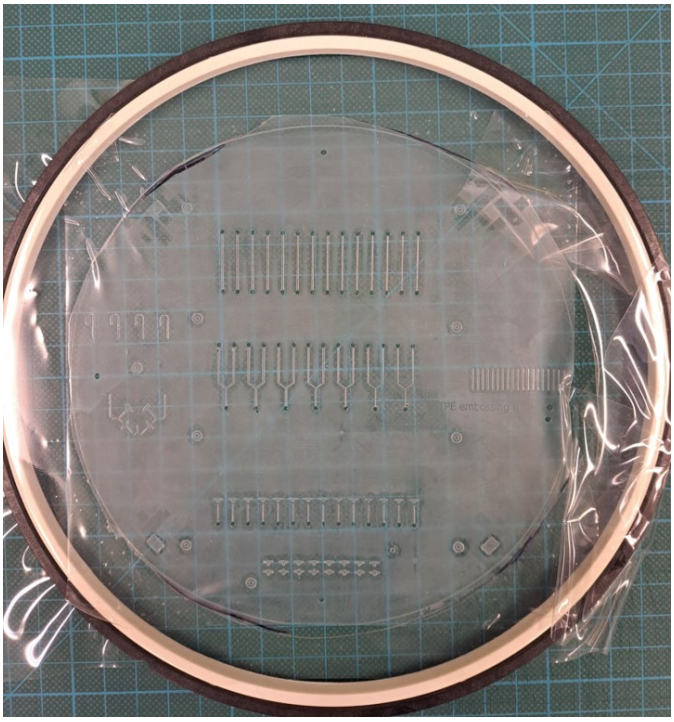

Figure 22: This image shows the TPE attached to a plastic film which is stretched on an expansion ring.

The TPE in the expansion ring was then precisely stacked on the top PS plate with the embossed features facing away from the top PS plate, after which the "bottom" PS plate is added on top. This stack is then hot pressed together so the PS and TPE bond together. This was done in a 4 step process in the hot press.

1. T0 (≈RT) and no pressure
2. T1 (>Tg) and no pressure for X1 seconds
3. T1 degrees and P1/P2 pressure for X2 seconds
4. T0 degrees and P1/P2 bar pressure for X3 seconds

After the combining of the stack was the extra TPE cut away. From the original pneumatic top PS plate was only one side micromilled. Now that the stack is complete the rest of the micromilling was done. First a program drilled all of the fluidic inlets, and after cleaning a drill connected the pneumatic lines in the stack with the fluidic inlets.

5.7 Fluidic priming

The first step of the fluidic characterisation was to prime the chips. This was done using the fluidic inlets. A mini luer is inserted in the inlets and tubing is connected to the mini luer. This tubing connects to a syringe with which colourless and blue coloured liquid was pushed through.

Due to the results of the fluidic priming no further fluidic characterisation was done. See section 6.1 for further explanation.

6 Results

The results of this research consist mostly of the depth and width characterisation of the features on the moulds, the embossed TPE and the stack itself. There are also some qualitative fluidic results.

6.1 PDMS and PC moulds

The characterisation of the features on the milled and embossed parts includes measurements of the depth and the width of the features. The first parts which were characterised where the milled PC mould and the casted PDMS mould. For each chip measurements were taken on predefined locations on each channel in the array. The results below show the average error of each of those locations compared to what was designed. This includes features of 50 μm depth and widths between 110 and 550 μm and these results are grouped per chip and the ruler. For the ruler what is measured is not the width of the features but the distance between them. This was designed to be 1150 μm and should give some insight in what the effects are if features are near the edge.

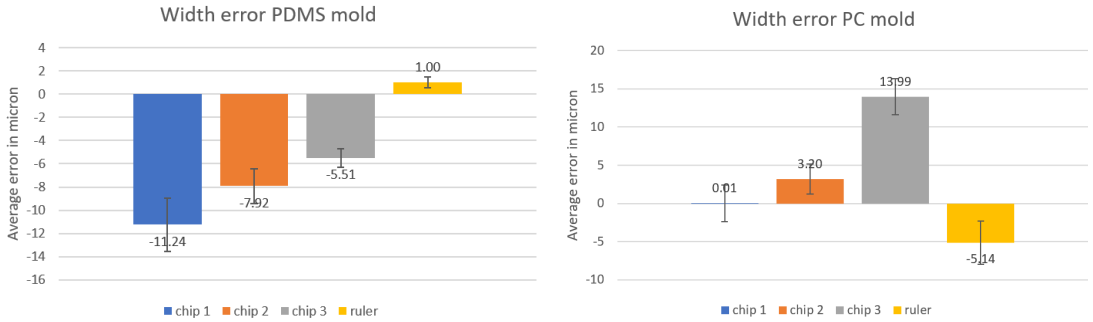

(a) (b)

Figure 23: This figure shows the average error of the width of the PDMS mould (a) and the PC mould (b) with a positive number being an increase in width.

Figure 23 (b) shows the average error of the widths which were measured on the PC mould and what was designed in Solidworks. What becomes apparent is that the micromilling machine produced channels with widths close to the widths which were intended. During the measuring of the widths of the PC mould the microscopy showed that there was a lot of burring. Burring are defects which are left over material near the edges of the micromilling. The not brittle material being milled left a lot of artifacts as seen in figure 24.

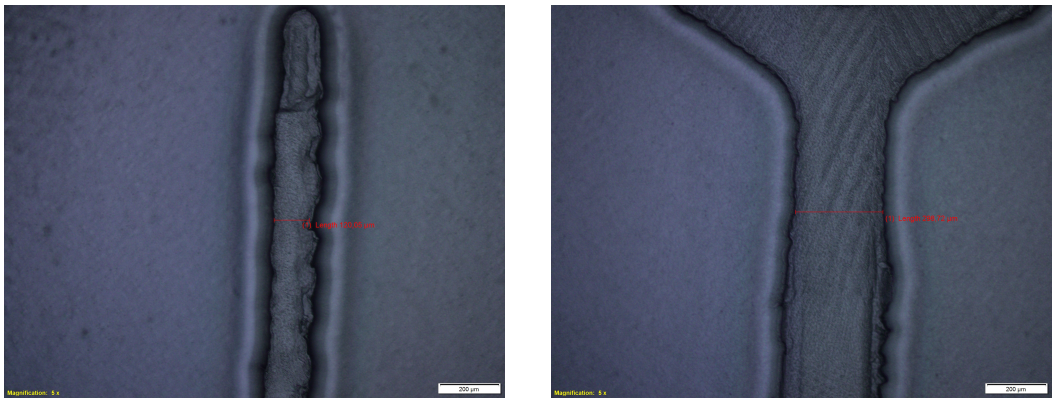

(a) (b)

Figure 24: These images show the burring with (a) being a thinner channel with more burring and (b) a wider channel with less burring.

These artefacts are more frequent with the thinner channels than with the wider channels, as seen in figure 24. The right image shows a wider channel where almost always it could be seen where the edge of the channel was. The smaller channels showed a lot of burring which often caused it to be unclear where the edges of the channels were. More examples of the burring making it harder to assess the width of the PC mould are shown below.

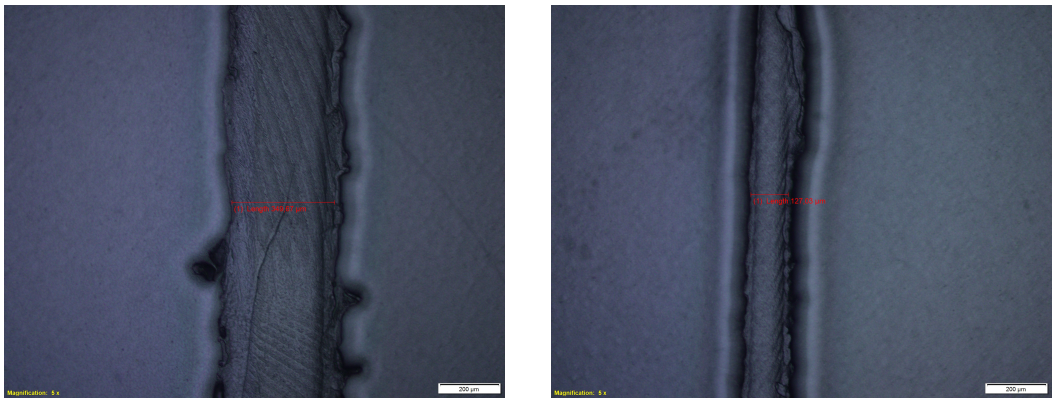

(a) (b)

Figure 25: These images show heavy burring around the channels on the PC mould.

The results shown in figure 23 (a) from the PDMS mould show that all of the widths have decreased from the original design. That the channels are less wide was to be expected as PDMS shrinks around 1-2% during casting [23]. The decrease of the width of the channels however exceeds this expected percentage, so it can be concluded that with this protocol the channels have decreased in width significantly. Especially chip one shows an average decrease of -11.24 which is 22.5% compared to the feature size. The characterisation via microscopy went well as no burring were blocking the view of the walls. This can be seen in figure 26.

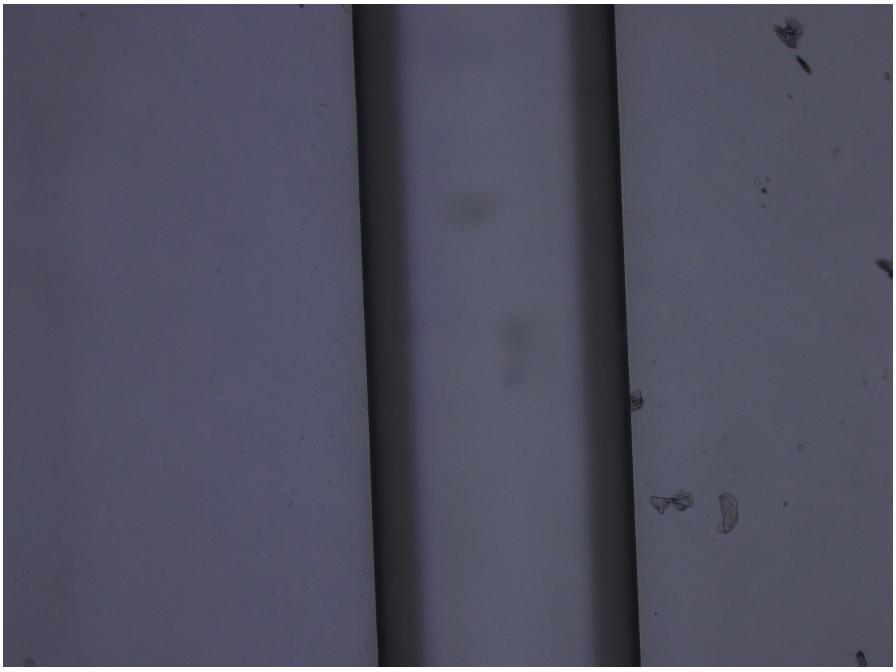

Figure 26: This image shows a channel on the PDMS mould.

The next characterisation for the moulds was done using the QV profilometer to measure the depth differences between the milled channels and the plate. Here it started to become more apparent that the QV profilometer was not producing consistent depth differences as the machine focused on the burrs as well. A hand profilometer was used to get the depth differences like mentioned in section 5.3. This was necessart for the PC mould and for the TPE.

What becomes clear from the graphs below graphs is that the depth differences for both moulds is close to what was designed. The biggest error is 3.96 μm for chip 2 of the PDMS mould which opposite to a designed depth difference of 50 μm is an error of around 8%.

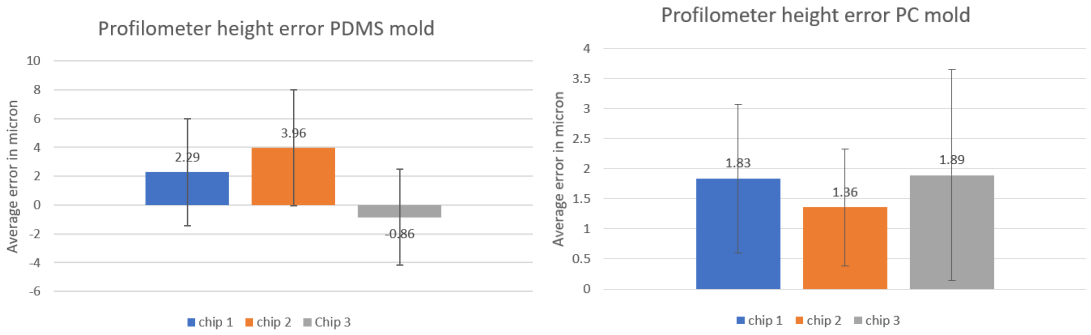

(a) (b)

Figure 27: This figure shows the average error of the depth difference of the features of the PDMS mould (a) and the PC mould (b) with a positive number being an increase in depth.

6.2 Embossed TPE

Both the width and the depth differences of the features on the embossed TPE were also characterised. Firstly two runs were performed with the PC mould. After these runs it became clear that the embossed TPE showed areas around the features where the TPE was clear. The TPE would be opaque if the embossing went correctly as the TPE was heated enough till above its Tg to start to reflow around the features. When the TPE reflows against the PC then the rougher patterning left by the pathing of the micromilling is transferred to the TPE causing the TPE to turn more opaque. This implies that with the current Hot embossing settings the TPE does not reflow completely around the features.

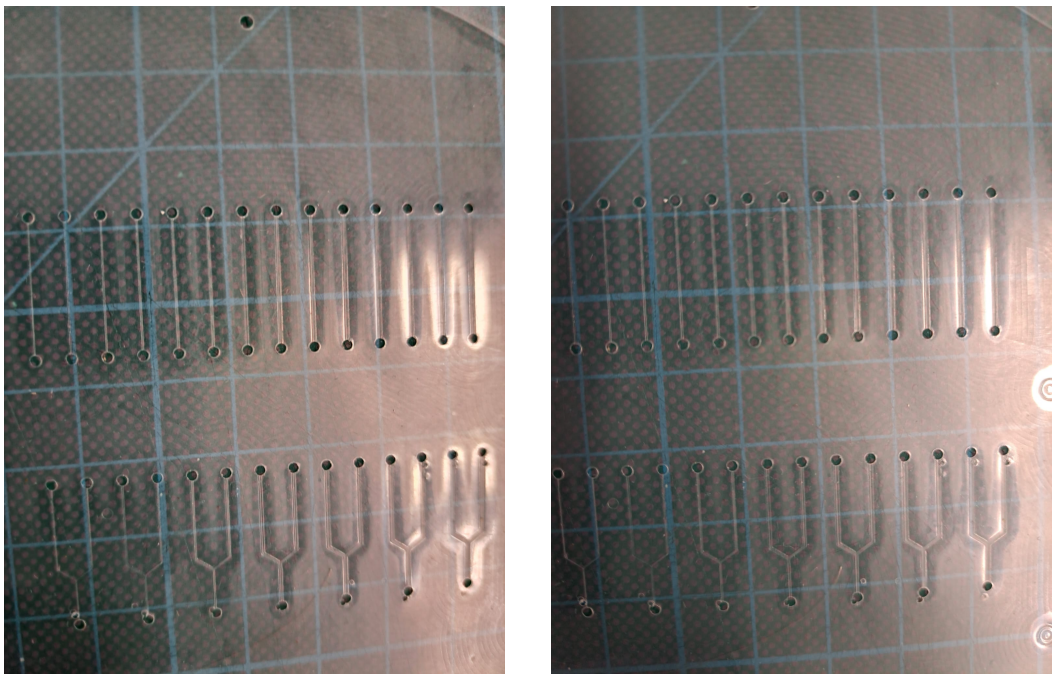

(a) (b)

Figure 28: These images show the difference in opacity near the features on the embossed TPE from the PC mould with (a) being from a lower temperature run and (b) from a higher temperature run.

This originates from the fact that the PC mould's surface is not smooth since the micromilling could not achieve optical quality/grade finishing. This "shadowing" effect indicates that either the pressure was not high enough, or the temperature was to low. As the pressure was deemed high enough it was decided to increase the temperature. Another run of two embossings using the PC mould was done increasing the temperature in steps of 10 degrees. The results for these runs show the same shadowing effect as seen in figure 28 (b).
Because of the shadowing effect and the difficulty with the profilometer it was decided to continue with the PDMS mould's embossed TPE only. First microscopic characterisation showed that the The width characterisation of 2 runs of embossed TPE is shown below. The protocol which was uses was the same one as the last run of the PC mould with the highest temperature.

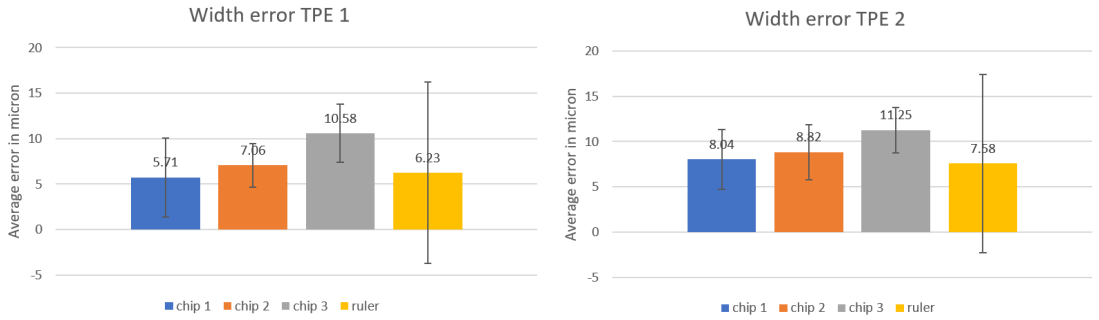

(a) (b)

Figure 29: This figure shows the average error of the widths of the features of 2 embossed TPE from the PDMS mould.

Figure 29 shows the results for the average width error of the channels for each chip. All the features show an increase of width, contradicting the decreased width of the PDMS mould. The profilometer results of the embossed TPE is shown below.

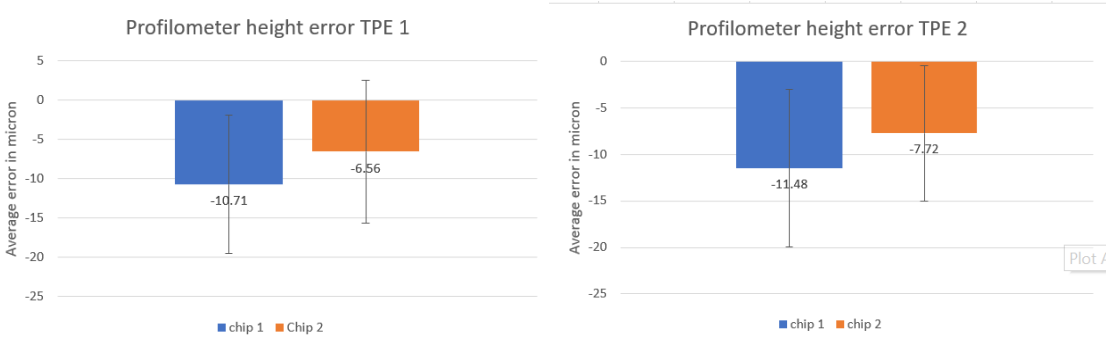

(a) (b)

Figure 30: This figure shows the average error of the depth difference of the features of 2 embossed TPE from the PDMS mould.

Figure 30 shows that both TPE have a decrease in depth difference between the channels and the plate surface. The results are consistent between the 2 runs with the same protocol. This data set was the first profilometer characterisation. At first was chip 3 not included but all subsequent characterisations did include chip 3. From these results it also becomes clear that there is a very large standard deviation for both data sets. This implies that the results vary greatly. Looking at the results shows that the results vary between around 25 μm up to around 75 μm.

6.3 Stack

Nearing the end of this project a single stack was manufactured consisting out of the pneumatic PS plate, the bottom PS plate and the first of the PDMS mould embossed TPE. This stack was first hot pressed with the pressure at P1 bar. After the fusion bonding it became apparent, during microscopic assessment, that there were large areas that did not bond properly. This is shown below in figure 31.

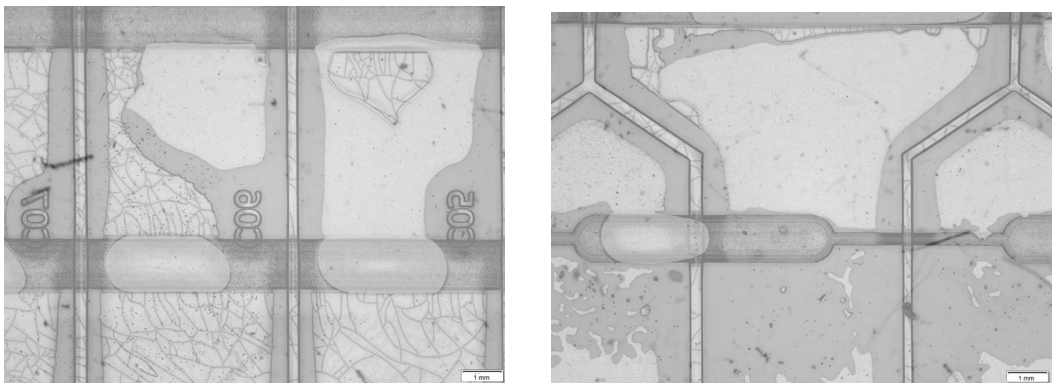

(a) (b)

Figure 31: These images shows parts of chip 1 (a) and chip 2 (b) with darker areas being bonded.

The stack was hot pressed once more after the microscopic assessment, now with P2 pressure. This showed to increase the bonding but still far from complete bonding.

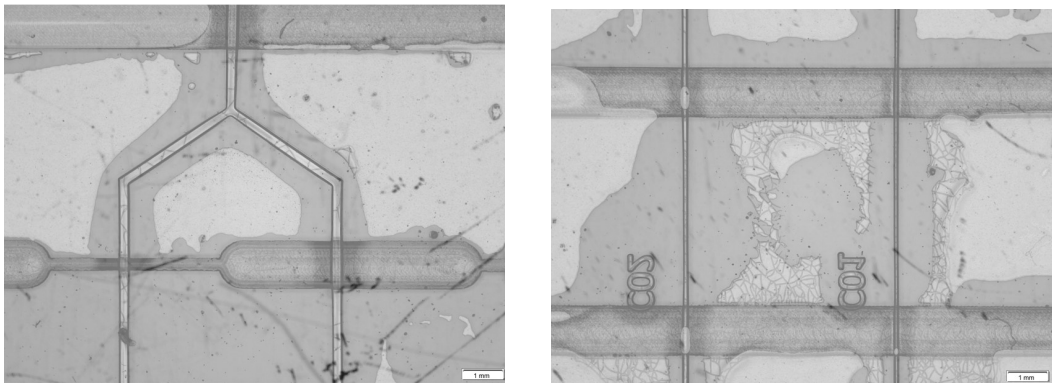

(a) (b)

Figure 32: These images shows parts of chip 1 (a) and chip 2 (b) with darker areas being bonded.

Figure 32 shows that the bonding is not complete yet, but the bonding does envelop the channels completely. Due to the bonding around the channels and time constraints, no further repeat of the fusion bonding process was performed.

The widths of the features in the stack were then characterised and the results are shown below.

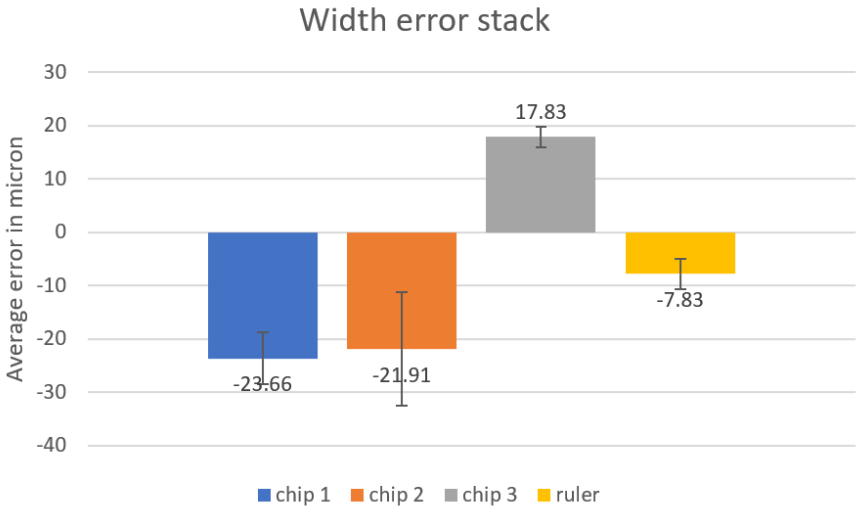

Figure 33: This figure shows the average error of the widths of the stack

What becomes apparent is that for chip 1, chip 2 and the ruler the widths of the channels decreased. Unlike the width results of the TPE before the assembly of the stack are the results of the third chip the odd one out, increasing in width rather than decreasing.

During microscopic assessment it became clear that the features on the third chip were misaligned.

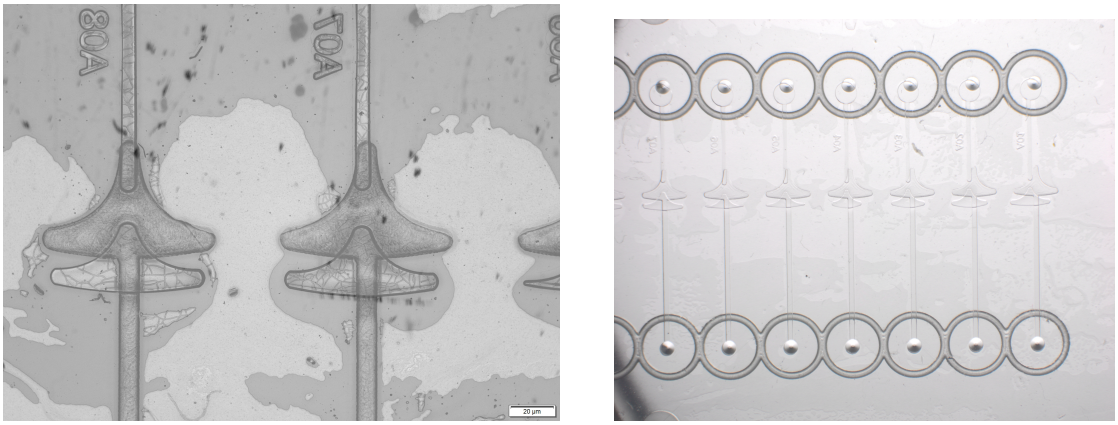

Figure 34: These images show chip 3 and the misalignment of the TPE and milled PS features.

As the other features did not seem to be misaligned this could explain the different results shown in figure 33. The misalignment of the features could cause the TPE to fold and increase the depth difference together with the burring so the third chip could not bond properly.

6.4 Fluidic priming

As mentioned before was a single stack manufactured nearing the end of the project. Fluidic priming was performed on both chip 1 and chip 2. The rest of the features did not have their inlets finalised and were not primed due to time constraints. What became quickly apparent is that the fluidic embossed channels were connected to the pneumatic channels.

Blue liquid was used for visualisation purposes and microscopic assessment shows clearly that blue liquid enters into all three of the pneumatic channels. This implies that the fluidic and pneumatic layers were connected. What did become apparent is that the fluid did follow the embossed channels before entering the pneumatic channels. The fluid passed from the fluidic to the pneumatic side where the two channels cross. This shows that Hot embossed channels work, but that the method of use for the valves is incorrect.

7 Discussion

7.1 Mould design

The designing of the mould was a gradual learning process. Many versions were created and checked and improved upon with the colleagues of Micronit. The locations and shape of the alignment markers for example went through a few versions until the circular design was chosen. The design of the moon shape cavities and which feature of that shape to change for the array was a difficult process, but eventually after many versions a final design was chosen.

Learning SolidWorks for designing a microfluidic device from the ground up was a process and a lot was personally learned during the many iterations. This project has also been a process for Micronit concerning the work for embossing and bonding the TPE. Another detail for example to improve the design was the use of 3D program extensions of SolidWorks to have the channels in chip 1 and 2 be rounded for the PC mould. This was not possible for the third chip as it could interfere with the check valves movement.
In the end a complex file was made with different configurations for the replica, the pneumatic side PS plate, the bottom PS plate and a separate body consisting out of the mould replica.

7.2 Micromilling and shallow alignment

The micromilling process is one which required trial and error. The code generation from SolidWorks is automatically loaded into the machine and needs to be checked or altered for different purposes, like disabling the spindle rotation for the drag knife.
Before starting the milling, the part was aligned to the coordinate system of the machine using the standard procedure programmed by Datron. This procedure uses a camera and a touch-probe to identify the center of the part.
The shallow alignment process was also one of trial and error. The features were 50 micron deep, and the probe had a tip of 1mm. A colleague within Micronit made a program called "Shallow alignment". This is a script developed by Micronit to allow the alignment on shallow pockets, using a probe with a size way bigger than the pocket. It was commonly used for hard thermoplastics so the use of the program was adapted to try on the soft TPE. This adaptation caused the process to often go wrong as the size of the features on the embossed TPE is near the bottom of the sensitivity of the Shallow alignment program. To ease this process some tape was cut and precisely applied to the 4 corner pockets to increase the depth of the edges.

7.3 Choosing the manufacturing methods

Before deciding that micromilling and glass etching were the manufacturing methods for the moulds, more methods were discussed. There have been meetings with MESA+ at the university for the possibility of using a direct writer lithography machine. This machine could accurately target areas for lithography but this was eventually discarded as the desired thickness for the design could not be achieved with the parameters the university allows for projects. 3D printing was also a manufacturing method which was discussed and researched at length. 3D printing is a versatile method but a machine with the resolution and process area at the same time compatible with our process was not available.

7.4 Manufacturing PDMS and PC moulds

The PDMS mould was created using the etched glass negative. The transfer from the design into the glass negative was mostly done in cooperation with colleagues of Micronit, and was produced using their own production facilities. 3 glass negatives were produced. The first run went awry as the PDMS was not able to seperate from the glass. The glass negative broke when more force was used and it was decided to recoat the other glass negatives. It is important to note that between the soft bake and the hard bake the PDMS and the glass negative were left for a week due to timing with the holidays. This could've caused the coating to go bad or the PDMS to crosslink over time causing the separation issues. The second run with the new coating and no waiting time in between went well and a third run was not necessary.

Manufacturing the PC mould turned out to be more difficult than expected. The malleable material left a lot of burring, even after thorough cleaning, which made subsequent characterisation harder. It is also hypothesized that the leftover burr and rough edges caused the shadowing effect seen in the embossed TPE. The burr has a height which pushes the TPE further away from the features. Due to time restrains no further TPE embossing runs with increased temperature or different iterations of the micromilling for the PC could with different settings were done to try to improve the used design.

7.5 Hot embossing

The starting settings used for the Hot embossing came from the expertise of Micronit. This meant that a lot of the settings were predefined from earlier researches. Hot embossing is a manufacturing method which Micronit has experience with, but not with features of on this small of a scale embossed into a TPE. It was decided to use the temperature as a variable keeping the other settings constant.

The first runs were performed on the PC mould as mentioned before. From the characterisation it became apparent that there was a lot of burring near the edges, especially with the smaller channels. After the iterations of temperature increases did not help the shadowing effect and difficulties measuring the depth mentioned in section 6.2, it was decided to continue with the PDMS mould due to timing constraints. The cause for the shadowing could be that the temperature or pressure settings were not optimal for the embossing on PC, but with the burr seen from the microscopic characterisation the cause could also be the increase of the depth of the edges of the channel. Edge artifacts like the burring could increase the depth of the features by a lot as the features are 50 μm deep, making it harder for the TPE to reflow until the foot of the channels.

7.6 fusion bonding

The settings used for the fusion bonding of the stack were also defined from Micronit's earlier experiences. Those researches included a higher stack with many more layers, so settings were used for this three layer design which had lower pressure and temperature. Micronit has experience with bonding TPE to thermoplastics but not to embossed thermoplastics.
Due to the deposition machine in the cleanroom needing maintenance for a while, together with other time constraints, only one stack could be made. This meant that for the bonding of the stack it was decided to start with low pressure settings and increase when necessary. The pressure started at P1 pressure, and was increased to P2 pressure after inspection showed areas which were not bonded. The same stack was hot pressed again, but still showed non-bonded areas. The areas around the features seemed to be bonded and, combining this with time constraints as it was the last week of the research, it was decided to try the fluidic characterisation on that final version of the stack.

7.7 Characterisation PDMS and PC moulds

The characterisation of the intermediary parts was a gradual process. The width measurements were often obstructed by burring or other artefacts, but qualitative checks showed that the width characterisation was consistent.
The PDMS mould widths in figure 23 (a) showed that the widths had decreased for all the features. This is partly in line with expectations as PDMS shrinks 1-2% during casting. However, the highest decrease in average width was 11.24 μm. This, opposite to the average widths of chip 1 being 330 μm, is a decrease of 3.4%. This is only slightly higher than expected.
Figure 23 (b) showed that the PC mould's features were close to what was designed with the exception of the third chip showing an average positive error of 13.99 μm. This exception of chip 3 showing other results is apparent in the PC mould, the embossed TPE from the PDMS mould and the stack as shown in figure 23 (b), figure 29 and figure 33 respectively. Chip 3 deviating from the other features does not seem to show in the width results of the PDMS mould. For the PC mould the difference could only be explained by a manufacturing error, as the micromilled channels are very similar to the other chip's channels. Chip 3 does have the moon shape features but what was characterised was the width of the channels leading to the moon shape, not the moon shape itself. It remains unclear what caused the manufacturing error.

The profilometer results in figure 27 show that both the PDMS mould and the PC mould have a depth difference between the bottom of the channels and the face of the PS plate which is very close to what was intended. The highest error of 3.96μm for chip 2 of the PDMS mould is still very close to what was designed. The PC mould did have trouble being characterised by the QV profilometer. As mentioned before an electrical device was used in combination with a microscope as a hand profilometer. The probable cause of the QV not working properly on the PC mould could be the burring near the edges. Research has shown that, depending on the speed and depth of the tool pathing in microdrilling, a burr can reach up to 100 μm in height from PC[34].

7.8 Characterisation Embossed TPE

What became apparent during the width characterisation of the embossed TPE is that the third chip, as mentioned before, was showing different results than the other features. In this case it could not be from the burring as seen with the PC mould, as the characterised TPE came from the PDMS mould which showed no shadowing effect. It is unclear why the third chips embossed channels in the stack averaged out to be less wide than designed opposite to the other features increasing in width, other than a manufacturing error.
The increase in width from the other features can be explained by the expansion due to increased temperature of PDMS. PDMS has an expansion coefficient of 310 $\mu m/m^{-1}C^{-1}$ [35]. This expansion causes the PDMS to expand during the embossing and makes the embossed features wider. This supports the results seen from the other features however contradicts the results of chip 3 even further.

Figure 30 shows the profilometer results for the embossed TPE. It shows that for both the embossed TPE the channels were more shallow than designed. This contradicts the expansion due to the thermal expansion of the PDMS mold. What could explain this decrease in feature depth is the fact that PDMS is a elastomeric material, and that the features on the PDMS mould could be squished down slightly during the pressurisation of the hot press. This would cause the feature depth to decrease and the channels to widen slightly. This increase in width further supports the results of chip 1, chip 2 and the ruler. What could explain these results further is the inaccuracy shown in the standard deviation. These runs with the profilometer were the first and it is possible that the method for the profilometer was not correct. This characterisation is recommended for repetition.

7.9 Stack

After the first run of fusion bonding the stack it became apparent that there were large areas which were not bonded. After a repeat fusion bonding with higher pressure more bonding occurred but still far from complete bonding as seen in figure 32. This implies that the settings for the fusion bonding were off, or other problems occurred in manufacturing. For example trapped air pockets could also cause problems with the bonding. No more iterations for the settings for the fusion bonding were tried due to time constraints. Due to the same time limitations no other stack was manufactured.

The results of the width characterisation of the channels in the stack show that the channels of chip 3 were not consistent with the rest of the features. Chip 1, chip 2 and the ruler all showed a decrease in channel width. This was to be expected, as the pressing of the stack could cause the embossed channel's edges to be pressed against the PS and bond. This bonding near the edges could lead to a decrease in channel width.
Possible causes for the third chip to have wider channels are the misalignment of the complex features of the check valves, namely the embossed moon shape in the TPE and the PS. This misalignment could be the cause of the TPE folding in places, which could increase the distance between the plate and the TPE. This increase could lead to the absence of pressure causing the channel's edges not to bond with the PS and keeping its original width. This however does not explain the increase in width seen in figure 33, and figure 31 shows us that there is bonding around the channels of the third chip so that implies that the distance between the two layers is not the issue. Next to possible manufacturing errors possibly involving the misalignment of the features on the third chip it is unclear why the results of third chip deviate from the rest of the features.

What could be the cause for the results to deviate is measurement precision. The features and distances which are characterised are very small. Both the QV and hand profilometer have shown inconsistent results. If the rack on which the hand profilometer was slightly slanted, or the QV profilometer auto focuses on the wrong layer, it could have been possible that a profilometer data set was off from reality. Routinely qualitative measurements were repeated to check if the profilometer provided consistent results, and if so the process was adjusted. Repetition will be required to show consistency and confirm the patterns which we discuss in this research.

7.10 Fluidic priming

Coloured liquid was used to visualize the fluidic priming of chip 1 and chip 2 the stack after the assembly. It became quickly apparent by microscopic assessment that the pneumatic channels and fluidic channels were connected in chip 1 and chip 2. This could have been caused by burring near the edges of the micromilled pneumatic channels cutting the TPE during the assembly and causing connections. As mentioned before can a burr reach 100 μm from PC[34].
As mentioned before microscopic assessment showed that the bonding of the stack was not complete. This lack of bonding could also have caused the fluid to pass the TPE to the side of the pneumatic channels already at the inlets. This however seemed to be not the case, because through microscopy was the blue liquid seen following the embossed channels before reaching the pneumatic channels and filling them up.

8 Conclusion

The goal of this research was to hot emboss microstructures onto TPE membranes using different kinds of moulds applied on down-scaling upscalable microfluidic elements. This research succeeded in replicating microstructures on TPE, with open discussions over some differences observed between the replica and the design. Embossed TPE from a PDMS mould casted on a glass etched negative and a micromilled mould were manufactured. The PDMS mould showed the best results as the PC showed a lot of burr and with the used method showed a "shadowing" effect around the features. This shadowing was attributed to the TPE not reflowing completely around the features. This could be the burring causing the TPE to be pushed further from the PC plate.
Characterisation for the width and the depth of the features has been performed on the three intermediary parts and their different iterations. The results show that the features on chip 3 deviated from the rest of the features in channel width error for the PC mould, the TPE and the stack. The deviated results from the TPE and the stack are contradictory. This could have been caused by manufacturing errors or the results deviate because of the measurement precision.
Fluidic priming with microscopy assessment showed that fluid was passing through the embossed channels correctly until reaching the crossover with the pneumatic channels. At the crossover were the two sides of the TPE connected. What could have possibly caused this is the cutting of the TPE by the edges of the pneumatic channels. No further fluidic characterisation could be done and due to time constraints no further stacks were manufactured. This research shows the compatibility of industrializable materials and processes used with the fabrication of active pneumatic elements, and sheds light on the first line of issues that need to be addressed to progress this further.

9 Future recommendations

The results of this research has proven that hot embossing fluidic channels has potential for the use in microfluidics. Recommendations for further research include repetition of manufacturing the intermediary parts and the final stack. Many different iterations of intermediary parts were manufactured, but due to time constraints and the many iterations no large scale quantitative assessment was done. After more testing future research could decide upon a final design and characterise on a larger volume of that design.
Recommended for future research is to continue on the fluidic priming and start the fluidic characterisation of the quake valves, check valves and side structures.
What is also recommended for future research is to further work on the settings for the fusion bonding and Hot embossing. Some iterations of settings were used but could definitely be improved upon.

References

[1] Elsbeth G B M Bossink, Anke R Vollertsen, Joshua T Loessberg-Zahl, Andries D Van Der Meer, Loes I Segerink, and Mathieu Odijk. Systematic characterization of cleanroom-free fabricated macrovalves, demonstrating pumps and mixers for automated fluid handling tuned for organ-on-chip applications. doi: 10.1038/s41378-022-00378-y. URL www.nature.com/micronano.

[2] Marc A. Unger, Hou Pu Chou, Todd Thorsen, Axel Scherer, and Stephen R. Quake. Monolithic microfabricated valves and pumps by multilayer soft lithography. *Science*, 288 (5463):113–116, 4 2000. ISSN 00368075. doi: 10.1126/SCIENCE.288.5463.113/ASSET/B92DF262-1777-4B31-B723-D0727EA2448E/ASSETS/GRAPHIC/SE1108400004.JPEG. URL https://www-science-org.ezproxy2.utwente.nl/doi/10.1126/science.288.5463.113.

[3] Pneumatic Valves - Alex Brosseau, Anthony Brouillard - OpenWetWare. URL https://openwetware.org/wiki/Pneumatic_Valves_-_Alex_Brosseau,_Anthony_Brouillard.

[4] Ritika Mohan, Benjamin R. Schudel, Amit V. Desai, Joshua D. Yearsley, Christopher A. Apblett, and Paul J.A. Kenis. Design considerations for elastomeric normally closed microfluidic valves. *Sensors and Actuators B: Chemical*, 160(1):1216–1223, 12 2011. ISSN 0925-4005. doi: 10.1016/J.SNB.2011.09.051.

[5] HUMIMIC Chip2 96-well Quick Guide. URL www.tissuse.com.

[6] Sébastien Cargou. Introduction about soft-lithography for microfluidics. *Elveflow*, 12 2020. URL https://www.elveflow.com/microfluidic-reviews/soft-lithography-microfabrication/introduction-about-soft-lithography-and-polymer-molding-for-microfluidic/.

[7] Fumihiro Sassa, Junji Fukuda, and Hiroaki Suzuki. Microprocessing of liquid plugs for bio/chemical analyses. *Analytical Chemistry*, 80(16):6206–6213, 8 2008. ISSN 00032700. doi: 10.1021/AC800492V. URL https://simplemicrofluidics.com/diy-microfluidics-prototyping/pdms-molded-microfluidics/.

[8] Ismail Emre Araci and Stephen R. Quake. Microfluidic very large scale integration (mVLSI) with integrated micromechanical valves. *Lab on a Chip*, 12 (16):2803–2806, 7 2012. ISSN 1473-0189. doi: 10.1039/C2LC40258K. URL https://pubs-rsc-org.ezproxy2.utwente.nl/en/content/articlehtml/2012/lc/c2lc40258khttps://pubs-rsc-org.ezproxy2.utwente.nl/en/content/articlelanding/2012/lc/c2lc40258k.

[9] A. R. Vollertsen, D. de Boer, S. Dekker, B. A.M. Wesselink, R. Haverkate, H. S. Rho, R. J. Boom, M. Skolimowski, M. Blom, R. Passier, A. van den Berg, A. D. van der Meer, and M. Odijk. Modular operation of microfluidic chips for highly parallelized cell culture and liquid dosing via a fluidic circuit board. *Microsystems & Nanoengineering 2020 6:1*, 6(1):1–16, 11 2020. ISSN 2055-7434. doi: 10.1038/s41378-020-00216-z. URL https://www.nature.com/articles/s41378-020-00216-z.

[10] The first autonomous, entirely soft robot. URL https://wyss.harvard.edu/news/the-first-autonomous-entirely-soft-robot/.

[11] Michael Wehner, Ryan L. Truby, Daniel J. Fitzgerald, Bobak Mosadegh, George M. Whitesides, Jennifer A. Lewis, and Robert J. Wood. An integrated design and fabrication strategy for entirely soft, autonomous robots. *Nature 2016 536:7617*, 536(7617):451–455, 8 2016. ISSN 1476-4687. doi: 10.1038/nature19100. URL https://www.nature.com/articles/nature19100.

[12] PhysioMimix® Liver plate - CN Bio. URL https://cn-bio.com/consumables/multi-chip-plates/physiomimix-liver-plate/.

[13] Nicoló Milani, Neil Parrott, Daniela Ortiz Franyuti, Patricio Godoy, Aleksandra Galetin, Michael Gertz, and Stephen Fowler. Application of a gut–liver-on-a-chip device and mechanistic modelling to the quantitative in vitro pharmacokinetic study of mycophenolate mofetil. *Lab on a Chip*, 22(15):2853–2868, 7 2022. ISSN 14730189. doi: 10.1039/D2LC00276K. URL https://pubs.rsc.org/en/content/articlehtml/2022/lc/d2lc00276khttps://pubs.rsc.org/en/content/articlelanding/2022/lc/d2lc00276k.

[14] Materials and Manufacturing Processes ISSN: (Print) (Online) Journal homepage: https://www.tandfonline.com/loi/lmmp20 Recent developments in hot embossing-a review Swarup S. Deshmukh & Arjyajyoti Goswami. 2020. doi: 10.1080/10426914.2020.1832691. URL https://www.tandfonline.com/action/journalInformation?journalCode=lmmp20.

[15] (PDF) Optimization of Hot Embossing Process for Fabrication of Microfluidic Devices. URL https://www.researchgate.net/publication/279970861_Optimization_of_Hot_Embossing_Process_for_Fabrication_of_Microfluidic_Devices.

[16] Tung Yi Lin, Truong Do, Patrick Kwon, and Peter B. Lillehoj. 3D printed metal molds for hot embossing plastic microfluidic devices. *Lab on a Chip*, 17 (2):241–247, 1 2017. ISSN 1473-0189. doi: 10.1039/C6LC01430E. URL https://pubs.rsc.org/en/content/articlehtml/2017/lc/c6lc01430ehttps://pubs.rsc.org/en/content/articlelanding/2017/lc/c6lc01430e.

[17] S. H. Ng and Z. F. Wang. Hot roller embossing for microfluidics: Process and challenges. *Microsystem Technologies*, 15(8):1149–1156, 8 2009. ISSN 09467076. doi: 10.1007/S00542-008-0722-0/FIGURES/12. URL https://link-springer-com.ezproxy2.utwente.nl/article/10.1007/s00542-008-0722-0.

[18] Wheatstone Bridge Circuit and Theory of Operation. URL https://www.electronics-tutorials.ws/blog/wheatstone-bridge.html.

[19] Soft Lithography for Microfluidics: a Review — Request PDF. URL https://www.researchgate.net/publication/242663793_Soft_Lithography_for_Microfluidics_a_Review.

[20] DATRON neo - Simple, Easy CNC Machining - DATRON Dynamics. URL https://www.datron.com/cnc-machines/datron-neo/.

[21] Jose L. Sanchez Noriega, Nicholas A. Chartrand, Jonard Corpuz Valdoz, Collin G. Cribbs, Dallin A. Jacobs, Daniel Poulson, Matthew S. Viglione, Adam T. Woolley, Pam M. Van Ry, Kenneth A. Christensen, and Gregory P. Nordin. Spatially and optically tailored 3D printing for highly miniaturized and integrated microfluidics. *Nature Communications 2021 12:1*, 12(1):1–13, 9 2021. ISSN 2041-1723. doi: 10.1038/s41467-021-25788-w. URL https://www.nature.com/articles/s41467-021-25788-w.

[22] Ciprian Iliescu, Hayden Taylor, Marioara Avram, Jianmin Miao, and Sami Franssila. A practical guide for the fabrication of microfluidic devices using glass and silicon. *Biomicrofluidics*, 6(1):016505, 3 2012. ISSN 19321058. doi: 10.1063/1.3689939. URL /pmc/articles/PMC3365353//pmc/articles/PMC3365353/?report=abstracthttps://www.ncbi.nlm.nih.gov/pmc/articles/PMC3365353/.

[23] James Friend and Leslie Yeo. Fabrication of microfluidic devices using polydimethylsiloxane. *Biomicrofluidics*, 4(2), 2010. ISSN 19321058. doi: 10.1063/1.3259624. URL /pmc/articles/PMC2917889//pmc/articles/PMC2917889/?report=abstracthttps://www.ncbi.nlm.nih.gov/pmc/articles/PMC2917889/.

[24] Simple Check Valves for Microfluidic Devices - Tech Briefs. URL https://www.techbriefs.com/component/content/article/tb/pub/briefs/mechanics-and-machinery/7954.

[25] Bobak Mosadegh, Chuan Hsien Kuo, Yi Chung Tung, Yu Suke Torisawa, Tommaso Bersano-Begey, Hossein Tavana, and Shuichi Takayama. Integrated elastomeric components for autonomous regulation of sequential and oscillatory flow switching in microfluidic devices. *Nature Physics 2010 6:6*, 6(6):433–437, 4 2010. ISSN 1745-2481. doi: 10.1038/nphys1637. URL https://www.nature.com/articles/nphys1637.

[26] Rectifier - Wikipedia. URL https://en.wikipedia.org/wiki/Rectifier.

[27] Sabu Thomas, A. R. Ajitha, and Maciej Jaroszewski. Polymer Blend Nanocomposites for Energy Storage Applications. *Polymer Blend Nanocomposites for Energy Storage Applications*, pages 1–550, 1 2023. doi: 10.1016/C2021-0-01800-9.

[28] Polycarbonate - Wikipedia. URL https://en.wikipedia.org/wiki/Polycarbonate.

[29] J. Rieger. The glass transition temperature of polystyrene. Results of a round robin test. *Journal of Thermal Analysis*, 46(3-4):965–972, 1996. ISSN 03684466. doi: 10.1007/BF01983614/METRICS. URL https://link.springer.com/article/10.1007/BF01983614.

[30] CleWin software – WieWeb software. URL https://wieweb.com/site/product-category/clewin-software/.

[31] SZX16 — Advanced Stereo Microscope — Olympus LS. URL https://www.olympus-lifescience.com/en/microscopes/stereo/szx16/.

[32] Microscope Image Analysis Software — OLYMPUS Stream — Olympus. URL https://www.olympus-ims.com/en/microscope/stream2/.

[33] Mitutoyo, Product family: Quick Vision WLI. URL https://shop.mitutoyo.nl/web/mitutoyo/en_NL/mitutoyo/Quick%20Vision%20WLI/Quick%20Vision%20White%20Light%20Interferometer/index.xhtml;jsessionid=AD3BF0795EA5CCBEEA6CDC9ED1857C10.

[34] Craig Hanson, Pratik Hiwase, Xingbang Chen, M. P. Jahan, Jianfeng Ma, and Greg Arbuckle. Experimental investigation and numerical simulation of burr formation in micro-milling of polycarbonates. 34:293–304, 2019. ISSN 23519789. doi: 10.1016/J.PROMFG.2019.06.153. URL https://www.researchgate.net/publication/334557340_Experimental_investigation_and_numerical_simulation_of_burr_formation_in_micro-milling_of_polycarbonates.

[35] Yun Xiao, Boyang Zhang, Anne Hsieh, Nimalan Thavandiran, Cristina Martin, and Milica Radisic. Microfluidic Cell Culture Techniques. *Microfluidic Cell Culture Systems*, pages 303–321, 2012. doi: 10.1016/B978-1-4377-3459-1.00012-0.